

Article

CFD Simulation of Hydrogen Sulfide (H₂S) Desulfurization Using Ionic Liquids and Graphene Oxide Membrane

Alon Davidy 

Independent Researcher, Petach-Tiqwa 4942136, Israel; alon.davidy@gmail.com; Tel.: +972-03-9049118

Abstract: Hydrogen sulfide (H₂S) is considered a toxic and corrosive gas, commonly found in natural gas, crude oil, and other fossil fuels. This corrosive gas may lead to stress corrosion cracking (SCC). This phenomenon is caused by the combined influence of tensile stress and a corrosive environment. This may lead to the sudden failure of normally ductile metal alloys, especially at an elevated temperature. Desulfurization is the process of removing H₂S from these fuels to reduce their harmful environmental and health impacts. Ionic liquids (ILs) have shown great potential for application as liquid absorbents for H₂S extraction because of their advantages such as non-volatility, functionality, high carbon solubility and low energy requirements for regeneration. The proposed hydrogen sulfide extraction system consists of a tube, membrane and shell. 1-ethyl-3-methylimidazolium (emim)-based ionic liquids with bis-(trifluoromethyl) sulfonylimide (NTf₂) anion has been selected due to its high H₂S diffusion coefficient. Functionalized graphene oxide (GO) advanced membranes have been employed in this design. In this research, H₂S extraction with ionic liquids has been numerically studied. The COMSOL finite element and multi-physics code has been employed to solve the continuity, turbulent fluid flow (k-ε model), and transient diffusion equations. For small time periods, there is sharp gradient in H₂S concentration profile inside the shell section. This is because the diffusion coefficient of H₂S in the ionic liquid is very small and the shell section is much thicker than the membrane. It has been determined that H₂S is absorbed almost completely by ionic liquids after a time period of 30,000 s.

Keywords: hydrogen sulfide; desulfurization; ionic liquid; COMSOL multiphysics code; Reynolds average Navier–Stokes (RANS); diffusion equation; continuity equation



Citation: Davidy, A. CFD Simulation of Hydrogen Sulfide (H₂S) Desulfurization Using Ionic Liquids and Graphene Oxide Membrane. *Fuels* **2023**, *4*, 363–375. <https://doi.org/10.3390/fuels4030023>

Academic Editors: Barbara Apicella and Giovanna Ruoppolo

Received: 25 June 2023

Revised: 31 July 2023

Accepted: 18 August 2023

Published: 4 September 2023



Copyright: © 2023 by the author. Licensee MDPI, Basel, Switzerland. This article is an open access article distributed under the terms and conditions of the Creative Commons Attribution (CC BY) license (<https://creativecommons.org/licenses/by/4.0/>).

1. Introduction

Hydrogen sulfide (H₂S) is considered toxic and is commonly found in natural gas, crude oil, and other fossil fuels. This corrosive gas may also lead to stress corrosion cracking (SCC). This phenomenon is caused by the combined influence of tensile stress and a corrosive environment. This may lead to the sudden failure of normally ductile metal alloys, especially at an elevated temperature [1]. Desulfurization is the process of removing H₂S from these fuels to reduce their harmful environmental and health impacts.

1.1. Literature Review of Conventional Desulfurization Methods

The most common method of H₂S desulfurization is the Claus process, which involves the following steps [2,3]:

- (1) The raw gas containing H₂S is burned with oxygen to produce sulfur dioxide (SO₂).
- (2) The SO₂ is then reacted with more H₂S in the presence of a catalyst to produce elemental sulfur (S) and water (H₂O).
- (3) The sulfur is then removed and the gas is purified.

Another method of H₂S desulfurization is through the use of biological processes, such as bio-desulfurization, which uses microorganisms to metabolize H₂S into sulfur. H₂S desulfurization is an important process in the oil and gas industry, as it helps to reduce the environmental and health impacts of fossil fuel production and use.

Yu et al. reviewed the current literature studies on the H₂S extraction processes by using zeolite catalysts. Their review includes experimental and simulation studies [4]. Valesco et al. implemented an iron-redox biological process in order to remove hydrogen sulfide (H₂S) from biogas emitted from a closed landfill [5]. Almenglo et al. installed a pilot bio-trickling filter (BTF) in a wastewater treatment plant in order to treat real biogas [6]. Tayar et al. studied different types of low-cost packing materials in columns in order to reduce the initial and operational costs of biogas bio-desulfurization [7]. There are several available methods for hydrogen sulfide removal, depending on the specific application and the desired level of removal. Some commonly used techniques are presented as follows:

Chemical oxidation: Hydrogen sulfide can be oxidized to elemental sulfur or sulfate using chemical oxidants such as chlorine, hydrogen peroxide, or ozone. This process converts H₂S into less harmful substances that can be easily separated or further treated.

Biological desulfurization: Biological processes employ specialized bacteria to metabolize hydrogen sulfide and convert it into elemental sulfur or sulfate. This method is often used in wastewater treatment plants and other biological treatment systems.

Adsorption: Adsorption involves the use of solid materials, such as activated carbon or specialized adsorbents, to capture and remove hydrogen sulfide. The gas molecules adhere to the surface of the adsorbent material, effectively removing them from the surrounding air or water.

Chemical scrubbing: In chemical scrubbing, a liquid scrubbing agent is used to absorb hydrogen sulfide gas. Common scrubbing agents include alkaline solutions, such as sodium hydroxide or sodium carbonate. The hydrogen sulfide reacts with the scrubbing agent to form a non-volatile compound that can be easily separated.

Catalytic conversion: Catalytic converters are used in some industrial processes to convert hydrogen sulfide into elemental sulfur. These converters contain catalysts that facilitate the chemical reaction, resulting in the formation of solid sulfur that can be collected and removed.

It is important to select the appropriate hydrogen sulfide removal method based on factors such as the concentration of H₂S, the volume of gas or liquid to be treated, the desired level of removal, and the specific environmental and safety considerations of the application.

1.2. Literature Review of the Employment of Ionic Liquid for Extractive Desulfurization

At present, hydro-desulfurization (HDS) technology is widely applied in industry, in which sulfur compounds in fuel oils react with hydrogen in presence of catalysts [8] to produce hydrogen sulfide (H₂S) and H₂S is removed from fuel oils [9]. However, this advanced technology is facing some challenges, with more countries limiting the sulfur content in fuel oils to lower levels, even to zero [9]. It should be noted that alternative methods such as extraction, oxidation, adsorption and bio-desulfurization have been studied, among which extractive desulfurization (EDS) is one of the preferable methods because it can be carried out under mild and simple conditions, does not alter the chemical structure of the compounds in fuel oils and the extracted sulfur compounds can be re-used as raw materials. Ionic liquids (ILs) provide a new option for EDS. Different from traditional molecular solvents, ILs are entirely composed of cation and anion. They are not volatile. In addition to this, they have high thermal/chemical stability, tunable dissolving or extracting capabilities for inorganic or organic compounds, non-flammability, and recyclability [10]. Ionic liquids have been recognized as novel designable solvents, i.e., their properties can be tuned by altering their ionic structures to meet specific demands. Their cationic and anionic structures can be tailored to optimize their physico-chemical properties [11]. These desirable properties make them suitable for extraction in EDS.

Ionic liquids are a class of salts that are liquid at or near room temperature. They have unique properties such as low volatility, high thermal stability, and tunable physicochemical properties, which make them attractive for various applications, including hydrogen sulfide removal. Ionic liquids can be used as solvents or adsorbents to capture and remove

hydrogen sulfide from gas streams or liquid solutions. A few examples of ionic liquids applied for hydrogen sulfide removal are presented here:

Ammonium-based ionic liquids: Ionic liquids containing ammonium cations, such as tetraalkylammonium or alkylammonium, have been studied for hydrogen sulfide removal. These ionic liquids can chemically react with hydrogen sulfide, forming non-volatile ammonium sulfide compounds that can be separated from the gas or liquid phase.

Phosphonium-based ionic liquids: Ionic liquids containing phosphonium cations, such as trialkylphosphonium, have also shown potential for hydrogen sulfide removal. They can chemically react with hydrogen sulfide, leading to the formation of non-volatile phosphonium sulfide compounds that can be easily separated.

Imidazolium-based ionic liquids: Imidazolium-based ionic liquids are a widely studied class of ionic liquids. They have been investigated for hydrogen sulfide removal due to their high solubility for H₂S and ability to form hydrogen bonds with sulfur-containing compounds. These interactions facilitate the capture and removal of hydrogen sulfide from gas or liquid streams.

Pyridinium-based ionic liquids: Pyridinium-based ionic liquids have shown promise for hydrogen sulfide removal, particularly in liquid–liquid extraction processes. They can selectively extract hydrogen sulfide from liquid solutions, enabling its separation and removal.

The choice of an appropriate ionic liquid for hydrogen sulfide removal depends on factors such as its specific application, the gas or liquid matrix, the desired level of removal, and economic and environmental considerations. Further research and development are ongoing to optimize the performance and efficiency of ionic liquids in hydrogen sulfide removal processes.

EDS using ILs has been studied intensively. Wang and Zhang used an altered acidity and iron (III) concentration by varying molar ratios of FeCl₃·6H₂O to 1-butyl-3-methylimidazolium chloride ([bmim] Cl) in the synthesis of iron (III)-containing ionic liquids. It was found that 1-butyl-3-methylimidazolium tetrachloroferrate ([bmim] Fe(III)Cl₄) is highly reactive toward H₂S [12]. Abdullah et al. [13] have shown that the absorption capacity of sulfur compounds in ILs is strongly dependent on the chemical structures, physical properties and compactness between the cation and the anion of the ILs [14].

1.3. Scope and Novelty of This Paper

In this research, hydrogen sulfide extraction based on ionic liquids has been calculated. This paper includes the simulation of the hydrogen sulfide extraction system. COMSOL software was applied in order to solve the continuity, turbulent fluid flow (by applying k - ϵ model), and diffusion equations. This work is probably the first coupled CFD simulation of H₂S extraction based on ionic liquid system and the graphene oxide (GO) membrane. This system is shown in Figure 1.

In an oil refinery, hydrogen sulfide (H₂S) can be generated from various sources during the processing of crude oil. Some of the major sources of H₂S in an oil refinery include:

Crude oil: Hydrogen sulfide can naturally occur in crude oil deposits, and its concentration varies depending on the oil source. As crude oil is processed in the refinery, H₂S can be released from the oil stream.

Hydro-treating units: Hydro-treatment is a refining process that involves the use of hydrogen to remove impurities, such as sulfur compounds, from various refinery products, such as gasoline, diesel, and jet fuel. The removal of sulfur compounds results in the release of hydrogen sulfide gas.

Hydrocracking units: Hydrocracking is a process that converts heavy hydrocarbons into lighter products using hydrogen as a catalyst. During this process, sulfur-containing compounds are broken down, releasing H₂S.

Coking units: Coking units convert residual heavy oils into lighter products and petroleum coke. Sulfur compounds in the residual oils can decompose during coking, leading to the release of H₂S.

Sour water strippers: Sour water is generated in various refinery units that contain hydrogen sulfide and ammonia. Sour water strippers are used to remove H₂S from this water stream, and the stripped gas contains H₂S.

Delayed coker units (DCU): Delayed coking is a process that converts residual heavy oils into petroleum coke. As in coking units, sulfur compounds in the residual oils can decompose, generating H₂S.

Desulfurization units: Refineries may have desulfurization units that remove sulfur compounds from specific refinery streams. During this process, H₂S can be produced as a byproduct.

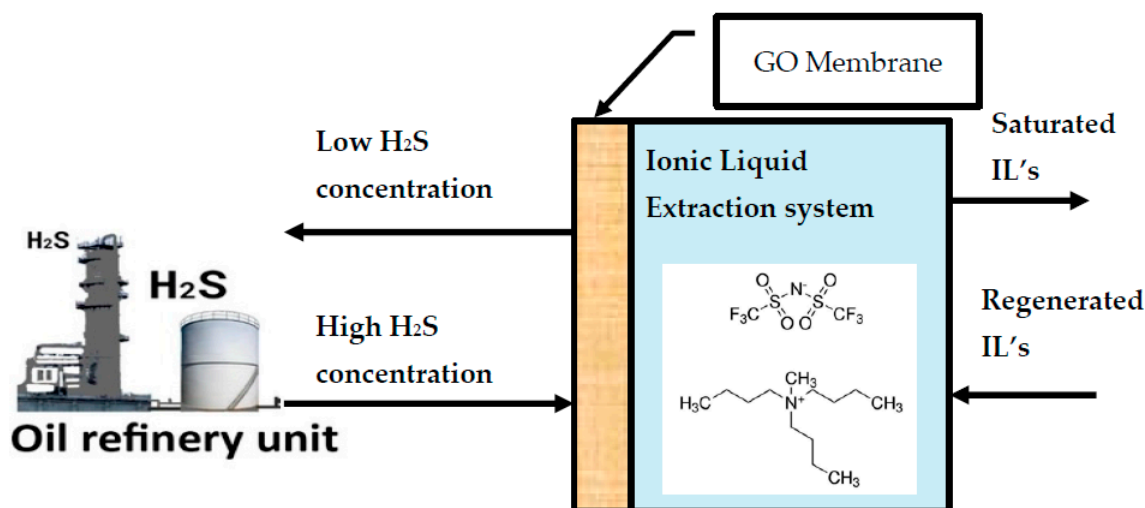


Figure 1. Schematics of the hydrogen sulfide extraction system.

As can be seen from Figure 1, the hydrogen sulfide is diffused inside the GO membrane absorbed by 1-ethyl-3-methylimidazolium (emim)-based ionic liquids with bis-(trifluoromethyl) sulfoniylmide (NTf₂) ionic liquid.

2. Materials and Methods

2.1. Diffusion Coefficients of Hydrogen Sulfide inside the Tube, Membrane and Shell Sections

1-ethyl-3-methylimidazolium (emim)-based ionic liquids with bis-(trifluoromethyl) sulfoniylmide (NTf₂) anion were selected due to their high H₂S diffusion coefficient. The diffusion coefficients of the H₂S inside the water ($D_{H_2S-water}$), ionic liquid and the functionalized graphene oxide (GO) membrane (D_{H_2S-GO}) and ionic liquid (D_{H_2S-IL}) are shown in Table 1 [14–16]. It should be noted that the H₂S diffusion coefficient inside graphene oxide (GO) is much higher than the H₂S diffusion coefficient inside Nafion112 [17].

Table 1. Diffusion coefficients of hydrogen sulfide in the water ($D_{H_2S-water}$), in the functionalized graphene oxide (GO) membrane (D_{H_2S-GO}) and the ionic liquid (D_{H_2S-IL}) [14–16].

Material Property	Value	Reference
$D_{H_2S-water}$	$17 \cdot 10^{-10}$ (m ² /s)	[16]
D_{H_2S-GO}	$20 \cdot 10^{-10}$ (m ² /s)	[15]
D_{H_2S-IL}	$8 \cdot 10^{-10}$ (m ² /s)	[14]

The GO membrane offers several advantages such as:

- (a) Graphene oxide membrane has an exceptionally high permeability to various gases and liquids. Its structure allows for the faster diffusion and transport of molecules compared to conventional membranes.
- (b) It is chemically stable and resistant to many corrosive substances, making it suitable for use in harsh environments.
- (c) It can be engineered to be selective for specific molecules or ions. By controlling the size and functional groups on the surface of the graphene oxide sheets, it can be tailored for different applications, such as water purification or gas separation.

2.2. Multiphysics Analyses of the Hydrogen Sulfide Extraction System

This subsection provides a numerical analysis of the hydrogen sulfide extraction system. Figure 2 shows the geometry of this system.

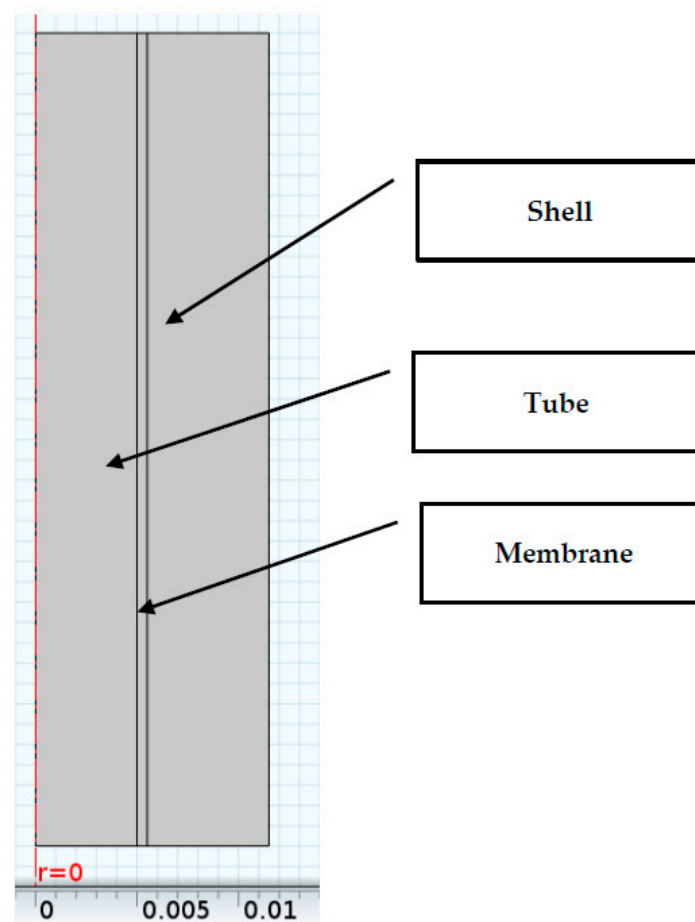


Figure 2. 2D plot of the hydrogen sulfide extraction system.

The tube radius is 5 mm, and its length is 40 mm. The membrane thickness is 0.5 mm. The shell thickness is 4 mm. COMSOL software was applied in this work. It solves the following governing equations:

- (a) Reynolds-averaged Navier–Stokes (RANS) and continuity equations. Wilcox ($k-\epsilon$) turbulence model was applied in the tube domain.
- (b) Convective mass transport equation in the tube domain.
- (c) Diffusion transport equations in the three domains (tube, membrane and the shell).

Reynolds-averaged Navier–Stokes (RANS) equations are a set of equations used in fluid dynamics to model the behavior of turbulent flows. They are derived from the Navier–Stokes equations, which describe the motion of fluid in terms of velocity, pressure, and other properties. The RANS equations incorporate the concept of turbulence by introducing additional terms that represent the effects of turbulence on the flow. Turbulence is characterized by chaotic, random fluctuations in velocity and pressure, which can significantly influence the overall flow behavior. However, directly solving the turbulent flow equations is computationally expensive and impractical for many engineering applications. In RANS, the equations are averaged over time, resulting in equations that represent the mean flow behavior with additional terms that account for the turbulent fluctuations. These additional terms are often modeled using turbulence models, which are mathematical models that provide closure for the turbulent terms in the equations. The choice of turbulence model depends on the specific flow conditions and the level of accuracy required.

2.2.1. Continuity and Fluid Flow Equations

The characteristic of a flow is often described by Reynolds number, which is defined as:

$$Re = \frac{\rho U d}{\eta}$$

where U is the velocity inside the tube and d is the tube diameter. The temperature of the water is 25 °C. ρ is the fluid density and η is the fluid viscosity. The inlet velocity, U , is 0.5 m/s. The pipe diameter, d , is 0.01 m. It has been assumed that a mixture of water and hydrogen sulfide is flowing inside the tube. Then, using standard values for water density and viscosity, the equation gives an approximate Reynolds number of 5000.

Since the Reynolds number of the flow inside the tube is greater than 2100 [18,19], this Reynolds is high enough to warrant the use of a turbulence. The k - ϵ model is often used in turbulence models for industrial applications. The COMSOL multiphysics code includes the standard k - ϵ model. This model introduces two additional transport equations and two dependent variables: the turbulent kinetic energy, k , and the dissipation rate of turbulence energy, ϵ . The turbulent viscosity is modeled by [20,21]:

$$\eta_T = \rho C_\mu \frac{k^2}{\epsilon} \tag{1}$$

C_μ is a model constant. The transport equation for k is [20]:

$$\rho \frac{\partial k}{\partial t} - \nabla \cdot \left[\left(\eta + \frac{\eta_T}{\sigma_k} \right) \nabla k \right] + \rho \mathbf{U} \cdot \nabla k = \frac{1}{2} \eta_T \left(\nabla \mathbf{U} + (\nabla \mathbf{U})^T \right)^2 - \rho \epsilon \tag{2}$$

The transport equation for ϵ is [20,21]:

$$\rho \frac{\partial \epsilon}{\partial t} - \nabla \cdot \left[\left(\eta + \frac{\eta_T}{\sigma_\epsilon} \right) \nabla \epsilon \right] + \rho \mathbf{U} \cdot \nabla \epsilon = \frac{1}{2} C_{\epsilon 1} \frac{\epsilon}{k} \eta_T \left(\nabla \mathbf{U} + (\nabla \mathbf{U})^T \right)^2 - \rho C_{\epsilon 2} \frac{\epsilon^2}{k} \tag{3}$$

The turbulent model constants in the above equations are determined from experimental data [20]. Their values are listed in Table 2.

Table 2. Turbulent model constants [20].

Material Property	Value
C_μ	0.09
$C_{\epsilon 1}$	1.44
$C_{\epsilon 2}$	1.92
σ_k	1.0
σ_ϵ	1.3

Solving these equations involves discretizing them into a computational domain and employing numerical methods to obtain approximate solutions. Computational fluid dynamics (CFD) simulations are commonly used to solve RANS equations. It is worth noting that while RANS equations are widely used, they have limitations. They assume that turbulence can be characterized by its mean properties and neglect the effects of small-scale turbulent fluctuations. For flows with complex turbulence behavior or flows near walls, more advanced turbulence models or approaches such as large-eddy simulation (LES) or direct numerical simulation (DNS) may be required to accurately capture the flow phenomena. The mass conservation transport equation is [20]:

$$\nabla \cdot \mathbf{u} = 0 \quad (4)$$

2.2.2. Mass Transfer Equations of the H₂S in the Tube, Membrane and the Shell Sections

The transient mass transfer equation for the tube section is shown in Equation (5) [18,20]:

$$\partial c_1 / \partial t + \nabla \cdot (-D_{H_2S-water} \nabla c_1 + c_1 \mathbf{u}) = 0 \quad (5)$$

The transient mass transfer equation for the membrane is shown in Equation (6) [18,20]:

$$\partial c_2 / \partial t + \nabla \cdot (-D_{H_2S-GO} \nabla c_2) = 0 \quad (6)$$

The transient mass transfer equation (it is assumed that the ionic velocity inside the shell can be neglected) for the shell section is shown in Equation (7) [18,20]:

$$\partial c_3 / \partial t + \nabla \cdot (-D_{H_2S-IL} \nabla c_3) = 0 \quad (7)$$

2.2.3. Boundary Conditions

The boundary conditions at the interface of the tube section and the membrane are provided by the following Equation [18,20]:

$$(-D_{H_2S-water} \nabla c_1 + c_1 \mathbf{u}) \cdot \mathbf{n} = -D_{H_2S-GO} \nabla c_2 \quad (8)$$

The boundary conditions at the interface at the membrane/shell section are provided by Equation (9) [18,20]. The H₂S concentration incoming to the extraction system is 1000 mol/m³ (see Equation (10)). The flow velocity inside the tube section is 0.5 m/s (see Equation (11)).

$$(-D_{H_2S-IL} \nabla c_3) \cdot \mathbf{n} = -D_{H_2S-GO} \nabla c_2 \quad (9)$$

$$c_1(0 < r < r_{in}, z = 0, t) = c_{in} \quad (10)$$

$$\mathbf{u}(0 < r < r_{in}, z = 0, t) = v_{in} \quad (11)$$

3. Results

3.1. CFD Results Obtained Using GO Membrane

The segregated solver was applied in order to solve the turbulent flow equation.

The convergence plot is shown in Figure 3.

According to Figure 3, the numerical errors decreased from 1 to 1·10⁻³. Figure 4 provides the velocity profile inside the tube section.

Figure 4 shows that the flow inside the tube section is a fully developed turbulent velocity profile [22]. Figure 5 provides a two-dimensional (2D) plot of the hydrogen sulfide concentration profile at t = 3000 s.

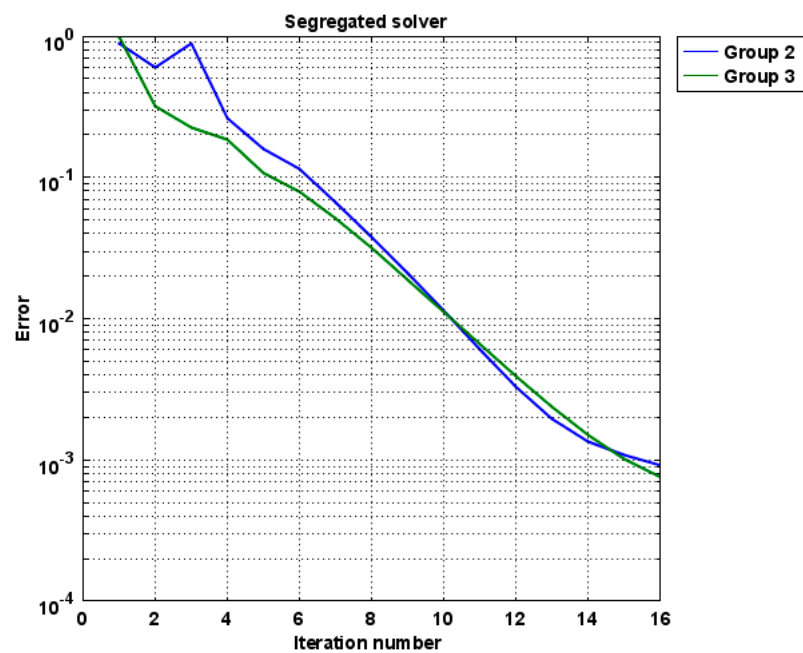


Figure 3. Convergence plot of the numerical turbulent Navier–Stokes equation.

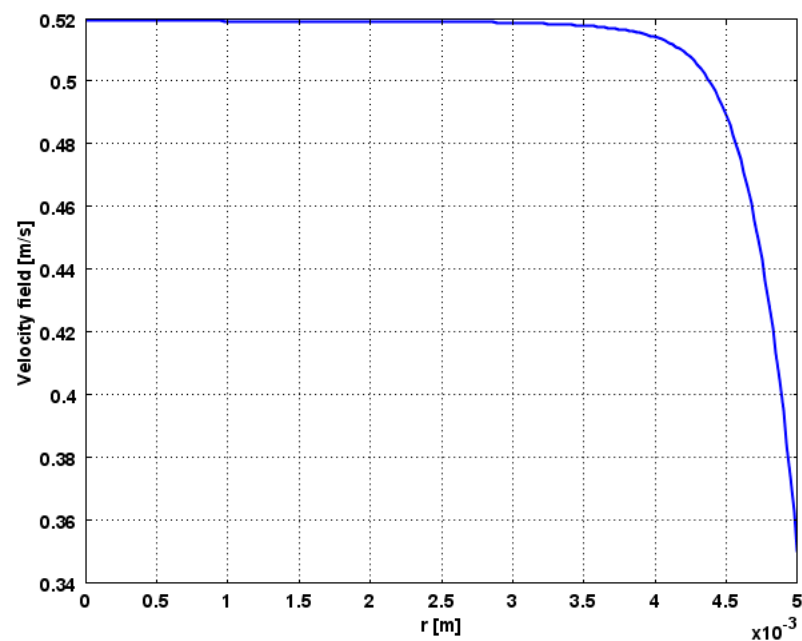


Figure 4. Flow velocity profile inside the tube.

Figure 5 shows that the hydrogen sulfide concentration decays along the radial axis. This is because the hydrogen sulfide is diffused into the membrane and the shell sections. Figure 6 provides a 3D plot of the hydrogen sulfide concentration profile at $t = 3000$ s.

Figure 6 shows that, for small time periods, there is sharp gradient in H_2S concentration profile inside the shell section. This is because the diffusion coefficient of H_2S in the ionic liquid is very small, and the shell section is much thicker than the membrane. Two CFD simulations with different elements (3708 and 14,832 elements) were performed using COMSOL Multiphysics. Figure 7 shows the instantaneous H_2S concentrations at the tube/membrane interface, at the membrane/IL interface and at the edge of the shell section (3708 elements).

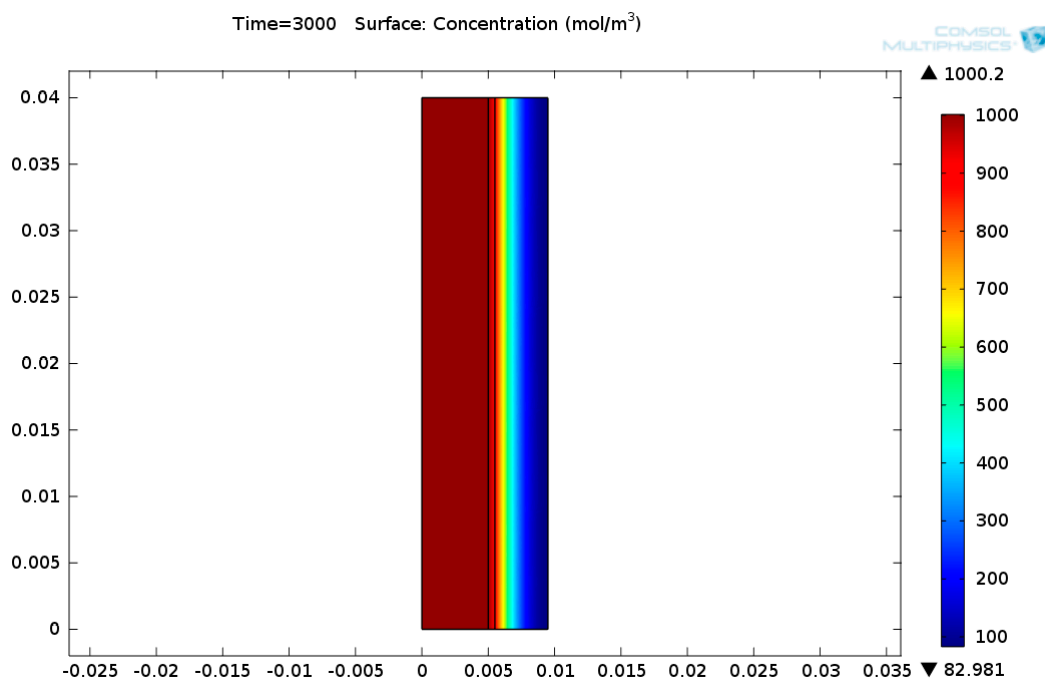


Figure 5. Two-dimensional plot of the hydrogen sulfide concentration profile.

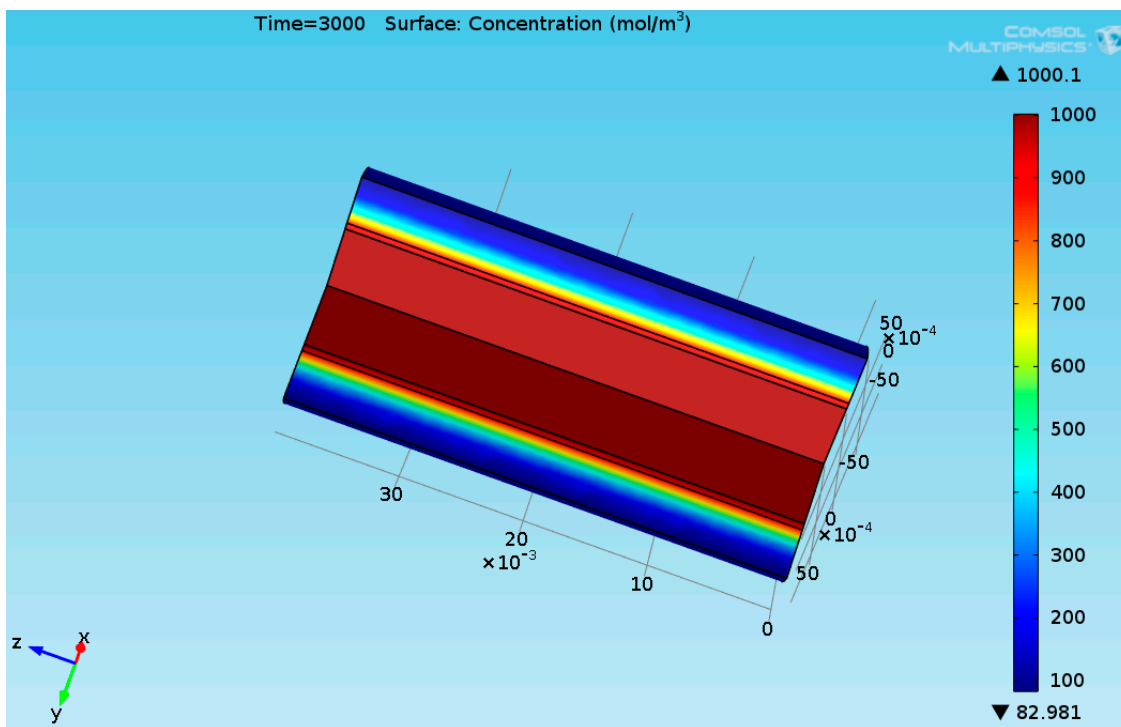


Figure 6. Three-dimensional plot of the hydrogen sulfide concentration profile.

It can be seen from Figure 7 that the H₂S is almost completely absorbed by the 1-ethyl-3-methylimidazolium (emim)-based ionic liquids with a bis-(trifluoromethyl) sulfonylimide (NTf₂) anion after a time period of 30,000 s. This is a function of the diffusion coefficients of the H₂S inside the membrane and the shell sections. Figure 8 provides the instantaneous H₂S concentrations at the tube/GO membrane interface, at the membrane/shell interface and at the edge of the shell section inside the extraction system (14,832 elements).

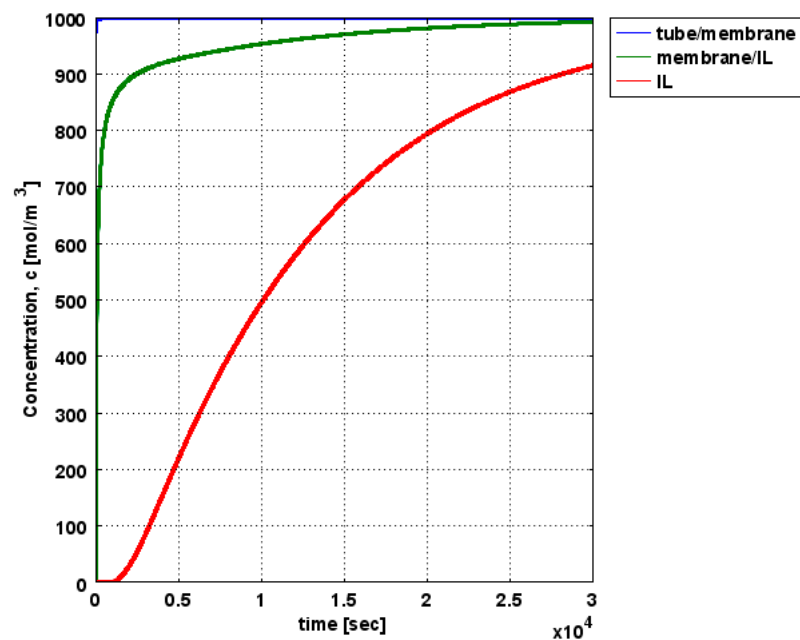


Figure 7. H₂S concentrations at different points of the extraction system (3708 elements).

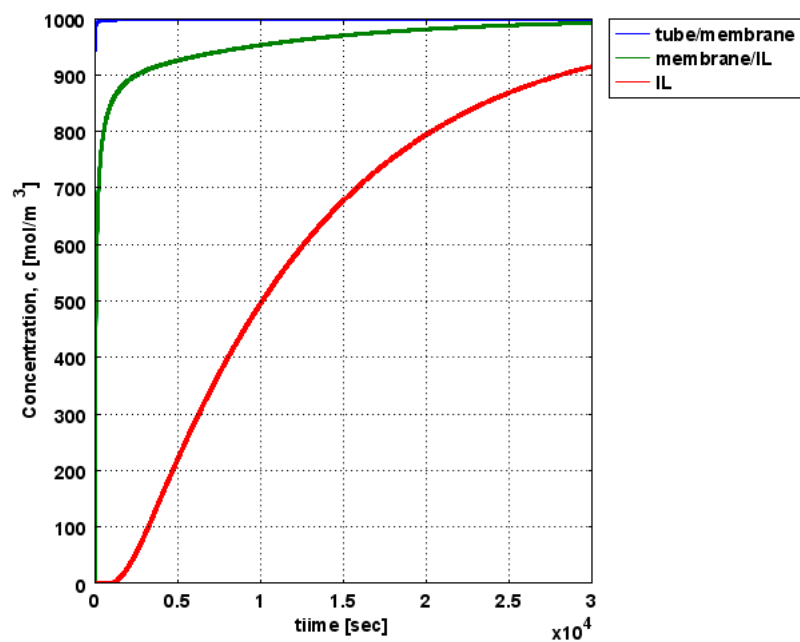


Figure 8. H₂S concentrations at different points of the extraction system (14,832 elements).

The H₂S concentration profiles obtained by the two CFD numerical simulations for 3708 and 14,832 elements are almost the same.

3.2. Validation of the CFD Result

The CFD results obtained using COMSOL software were validated against the analytical results. A closed-form solution was obtained for a constant surface concentration for semi-infinite mediums (this is valid for very short time periods). The analytical solution for this case may be obtained by applying a similarity variable, through which the diffusion equation may be transformed from a partial differential equation, involving two independent variables (x and t), to an ordinary differential equation expressed in terms

of the single similarity variable [23]. Figure 9 shows the analytical and numerical H₂S concentration results.

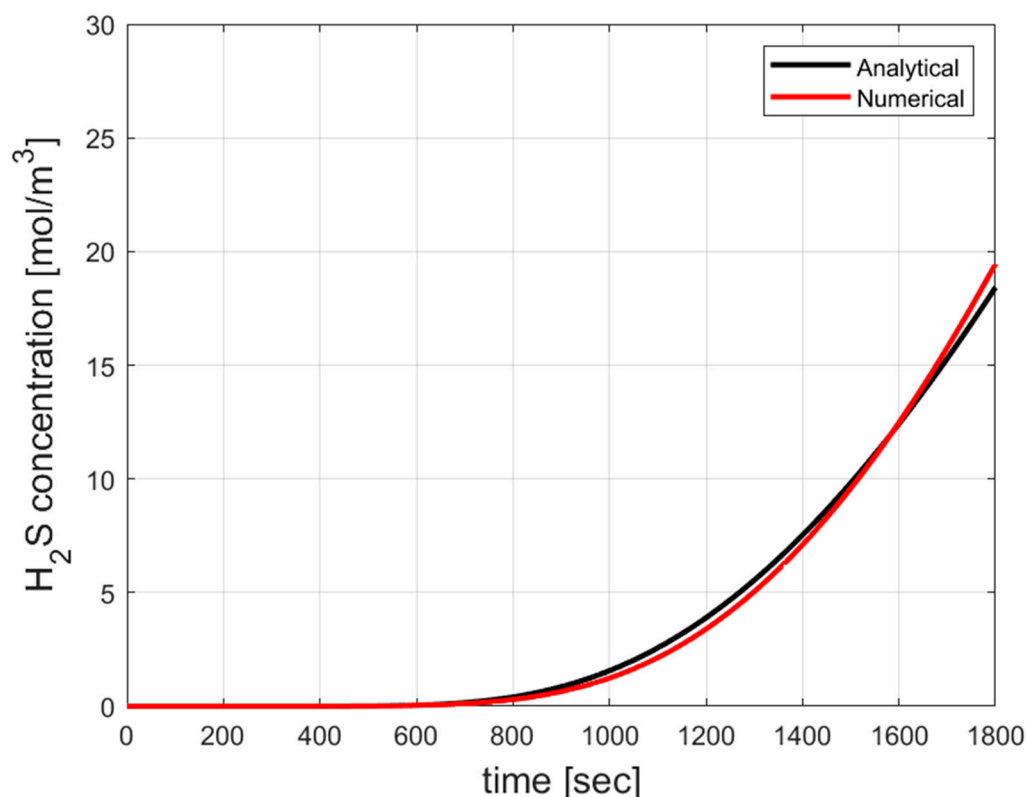


Figure 9. Analytical and numerical H₂S concentration results.

As can be seen from Figure 9, the analytical results are similar to the numerical results for short time periods. It should be noted that experimental results for this hydrogen sulfide extraction system have not been found. However, a similar model was recently developed for carbon-capture purposes [24]. The numerical results obtained for this similar system were favorably compared with the research work written by Sohaib et al. [25].

4. Conclusions

In this research, a hydrogen sulfide extraction system based on ionic liquids was calculated. The COMSOL finite element code solved the continuity, turbulent fluid flow (by applying a $k-\epsilon$ model), and mass transfer equations. This work is the first coupled CFD simulation of a H₂S extraction system based on an ionic liquid system and graphene oxide (GO) membrane.

The proposed hydrogen sulfide extraction system contains a tube, membrane and shell. 1-ethyl-3-methylimidazolium (emim)-based ionic liquids with bis-(trifluoromethyl) sulfonylimide (NTf₂) anion were selected due to their high H₂S diffusion coefficient. A functionalized graphene oxide (GO) membrane was employed in this design. This membrane offers several advantages such as:

- (a) The graphene oxide membrane has exceptionally high permeability to various gases and liquids.
- (b) It is chemically stable and resistant to many corrosive substances. It is suitable for use in harsh environments.
- (c) It can be engineered to be selective for specific molecules or ions.

It was determined that the H₂S is absorbed almost completely by the 1-ethyl-3-methylimidazolium (emim)-based ionic liquids with bis-(trifluoromethyl) sulfonylimide (NTf₂) anion after a time period of 30,000 s. This time period is a function of the diffusion

coefficients of the H₂S in the membrane and the ionic liquid. Two CFD simulations with different meshes (3708 and 14,832 elements) were carried out using the COMSOL multi-physics finite element code. It was found that the H₂S concentration profiles obtained from these two CFD simulations are almost the same. The CFD results obtained using COMSOL software were validated against the analytical results. A closed-form solution was obtained for a constant surface concentration for a semi-infinite medium (it is valid for very short time). The analytical solution for this case could be obtained by recognizing the existence of a similarity variable, through which the diffusion equation may be transformed from a partial differential equation involving two independent variables (x and t) to an ordinary differential equation expressed in terms of the single similarity variable. It was found that the analytical results are similar to the numerical results. This extraction system has several advantages:

- (a) Hydrogen sulfide (H₂S) is considered toxic. This system reduces hydrogen sulfide pollution.
- (b) It prevents stress corrosion cracking (SCC) to refine the piping system. H₂S SCC typically occurs when a metal is under tensile stress, which is stress that tends to stretch or elongate the material. The combination of tensile stress and exposure to H₂S can initiate and accelerate the cracking process. This phenomenon begins with the absorption of hydrogen atoms into the metal lattice. This can lead to the formation of hydrogen gas at specific locations, creating internal pressure that causes cracks to initiate and grow in the material. These cracks can ultimately lead to catastrophic failure of the component or structure if left unchecked. The severity of SCC is influenced by environmental factors, such as the concentration of H₂S, temperature, pressure, and the presence of other corrosive substances.

This extraction system can be further extended and can also include a spectral hydrogen sulfide infrared (IR) detection system.

Funding: This research has not received external funding.

Conflicts of Interest: The author declares no conflict of interest.

Abbreviations

CFD	Computational fluid dynamics
EDS	Extractive desulfurization
GO	Graphene oxide
HDS	Hydro-desulfurization
IL	Ionic liquid
RANS	Reynolds average Navier–Stokes
SCC	Stress corrosion cracking

Nomenclature

C	Concentration in [mole/m ³]
D	Diffusion coefficient in [m ² /s]
P	Pressure in [Pa]
p_{atm}	Atmospheric Pressure in [Pa]
\bar{R}	Gas constant (8.3143 J/(mole·K))
r_{in}	Inner radius of the tube [m]
r_{out}	Outer radius of the tube [m]
t	Time in [s]
$\mathbf{u}(u, v, w)$	Velocity vector in [m/s]
V	Velocity of the entering/leaving stream in [m/s]
Greek letters	
ρ	Density in [kg/m ³]

References

1. Anggabrata, D. In-Service Stress Corrosion Cracking of 316L Stainless Steel in H₂S. Available online: <https://www.corrosionpedia.com/in-service-stress-corrosion-cracking-of-316l-stainless-steel-in-h2s/2/7275> (accessed on 15 April 2023).
2. Zhang, X.; Wei, J.; Zhang, W. Tail Gas Hydro-Treating in a High H₂S Gas Plant. Available online: www.digitalrefining.com/article/1002598 (accessed on 15 April 2023).
3. Zahid, M.A.; Ahsan, M.; Ahmad, I.; Khan, M.N.A. Process Modeling, Optimization and Cost Analysis of a Sulfur Recovery Unit by Applying Pinch Analysis on the Claus Process in a Gas Processing Plant. *Mathematics* **2022**, *10*, 88. [CrossRef]
4. Yu, T.; Chen, Z.; Liu, Z.; Xu, J.; Wang, Y. Review of Hydrogen Sulfide Removal from Various Industrial Gases by Zeolites. *Separations* **2022**, *9*, 229. [CrossRef]
5. Velasco, A.; Franco-Morgado, M.; Revah, S.; Arellano-García, L.A.; Manzano-Zavala, M.; González-Sánchez, A. Desulfurization of Biogas from a Closed Landfill under Acidic Conditions Deploying an Iron-Redox Biological Process. *ChemEngineering* **2019**, *3*, 71. [CrossRef]
6. Almenglo, F.; Ramírez, M.; Cantero, D. Application of Response Surface Methodology for H₂S Removal from Biogas by a Pilot Anoxic Biotrickling Filter. *ChemEngineering* **2019**, *3*, 66. [CrossRef]
7. Tayar, S.P.; Guerrero, R.d.B.S.; Hidalgo, L.F.; Bevilacqua, D. Evaluation of Biogas Biodesulfurization Using Different Packing Materials. *ChemEngineering* **2019**, *3*, 27. [CrossRef]
8. Kabe, T.; Qian, W.H.; Ogawa, S.; Ishihara, A. Mechanism of Hydro-desulfurization of Dibenzothiophene on Co-Mo/Al₂O₃ and Co/Al₂O₃ Catalyst by the Use of Radioisotope ³⁵S Tracer. *J. Catal.* **1993**, *143*, 239–248. [CrossRef]
9. Abro, R.; Abdeltawab, A.A.; Al-Deyab, S.S.; Yu, G.; Qazi, A.B.; Gao, S.; Chen, X. A review of extractive desulfurization of fuel oils using ionic liquids. *R. Soc. Chem. Adv.* **2014**, *4*, 35302–35317. [CrossRef]
10. Chandra Srivastava, V. An evaluation of desulfurization technologies for sulfur removal from liquid fuels. *R. Soc. Chem. Adv.* **2012**, *2*, 759–783. [CrossRef]
11. Shafik El-Gendy, N.; Speight, J.G. *Handbook of Refinery Desulfurization*; CRC Press Taylor & Francis Group: Boca Raton, FL, USA, 2016.
12. Wang, J.; Zhang, W. Oxidative Absorption of Hydrogen Sulfide by Iron-Containing Ionic Liquids. *Energy Fuels* **2014**, *28*, 5930–5935. [CrossRef]
13. Abdullah, S.B.; Abdul Aziz, H.; Man, Z. *Ionic Liquids for Desulphurization: A Review*; Intechopen: London, UK, 2018. [CrossRef]
14. Shokouhi, M.; Sakhaeinia, H.; Jalili, A.H.; Zoghi, A.T. Ali, Experimental diffusion coefficients of CO₂ and H₂S in some ionic liquids using semi-infinite volume method. *J. Chem. Thermodyn.* **2019**, *133*, 300–311. [CrossRef]
15. Liu, Q.; Yang, Z.; Liu, G.; Sun, L.; Xu, R.; Zhong, J. Functionalized GO Membranes for Efficient Separation of Acid Gases from Natural Gas: A Computational Mechanistic Understanding. *Membranes* **2022**, *12*, 1155. [CrossRef] [PubMed]
16. Bahlake, A.; Farivar, F.; Dabir, B. New 3-dimensional CFD modeling of CO₂ and H₂S simultaneous stripping from water within PVDF hollow fiber membrane contactor. *Heat Mass Transfer* **2016**, *52*, 1295–1304. [CrossRef]
17. Sethuraman, V.A.; Khan, S.; Jur, J.S.; Andrew Haug, A.T.; Weidner, J.W. Measuring oxygen, carbon monoxide and hydrogen sulfide diffusion coefficient and solubility in Nafion membranes. *Electrochim. Acta* **2009**, *54*, 6850–6860. [CrossRef]
18. Bird, R.B.; Stewart, W.E.; Lightfoot, E.N. *Transport Phenomena*, 2nd ed.; John Wiley and Sons: Hoboken, NJ, USA, 2002.
19. Reynolds Number. Available online: <https://www.sciencedirect.com/topics/engineering/reynolds-number> (accessed on 25 June 2023).
20. COMSOL Multiphysics—Modeling Guide, Version 4.3b; COMSOL AB: Stockholm, Sweden, 2013.
21. Wilcox, D.C. *Turbulence modeling for CFD*, 3rd ed.; DCW Industries: La Cañada, CA, USA, 2006.
22. Salama, A. Velocity Profile Representation for Fully Developed Turbulent Flows in Pipes: A Modified Power Law. *Fluids* **2021**, *6*, 369. [CrossRef]
23. Incropera, F.P.; Dewitt, D.P.; Bergman, T.L.; Lavine, A.S. *Fundamental of Heat and Mass Transfer*, 6th ed.; John Wiley and Sons: Hoboken, NJ, USA, 2007.
24. Davidy, A. Numerical Study of CO₂ Removal from Inhalational Anesthesia System by Using Gas-Ionic Liquid Membrane. *ChemEngineering* **2023**, *7*, 60. [CrossRef]
25. Sohaib, Q.; Manuel Vadillo, J.; Gómez-Coma, L.; Albo, J.; Druon-Bocquet, S.; Irabien, A.; Sanchez-Marcano, J. Post-combustion CO₂ capture by coupling [emim] cation based ionic liquids with a membrane contactor; Pseudo-steady-state approach. *Int. J. Greenh. Gas Control* **2020**, *99*, 103076. [CrossRef]

Disclaimer/Publisher’s Note: The statements, opinions and data contained in all publications are solely those of the individual author(s) and contributor(s) and not of MDPI and/or the editor(s). MDPI and/or the editor(s) disclaim responsibility for any injury to people or property resulting from any ideas, methods, instructions or products referred to in the content.